THE FASEB JOURNAL

Interleukin 6 reduces vascular smooth muscle cell apoptosis via Prep1 and is associated with aging

Ilaria Cimmino[1] | Francesco Prisco[2] | Sonia Orso[1] | Ayewa L. Agognon[1] | Pasquale Liguoro[1] | Davide De Biase[2] | Nunzianna Doti[3] | Menotti Ruvo[3] | Orlando Paciello[2] | Francesco Beguinot[1] | Pietro Formisano[1] | Francesco Oriente[1]

[1]Department of Translational Medicine, Federico II University of Naples and URT "Genomic of Diabetes" of Institute of Experimental Endocrinology and Oncology, National Council of Research (CNR), Naples, Italy

[2]Department of Veterinary Medicine and Animal Production, Federico II University of Naples, Naples, Italy

[3]Institute of Biostructure and Bioimaging, National Research Council and Interuniversity Research Centre on Bioactive Peptides Naples, Naples, Italy

Correspondence
Pietro Formisano, Department of Translational Medicine, Federico II University of Naples and URT "Genomic of Diabetes" of Institute of Experimental Endocrinology and Oncology, National Council of Research (CNR), Via Pansini 5, 80131 Naples, Italy.
Email: fpietro@unina.it

Abstract

Aging exacerbates neointimal formation by reducing apoptosis of vascular smooth muscle cells (VSMCs) and induces inflammation within vascular wall. Prep1 is a homeodomain transcription factor which stimulates the expression of proinflammatory cytokines in aortic endothelial cell models and plays a primary role in the regulation of apoptosis. In this study, we have investigated the role of Prep1 in aorta of Prep1 hypomorphic heterozygous mice ($Prep1^{i/+}$) and in VSMCs, and its correlation with aging. Histological analysis from $Prep1^{i/+}$ aortas revealed a 25% reduction in medial smooth muscle cell density compared to WT animals. This result paralleled higher apoptosis, caspase 3, caspase 9 and p53 levels in $Prep1^{i/+}$ mice and lower Bcl-xL. Prep1 overexpression in VSMCs decreased apoptosis by 25% and caspase 3 and caspase 9 expression by 40% and 37%. In parallel, Bcl-xL inhibition by BH3I-1 and p53 induction by etoposide reverted the antiapoptotic effect of Prep1. Experiments performed in aorta from 18 months old WT mice showed a significant increase in Prep1, p16^{INK4}, p21^{Waf1} and interleukin 6 (IL-6) compared to youngest animals. Similar results have been observed in H_2O_2-induced senescent VSMCs. Interestingly, the synthetic Prep1 inhibitory peptide Prep1 (54–72) reduced the antiapoptotic effects mediated by IL-6, particularly in senescent VSMCs. These results indicate that IL-6-Prep1 signaling reduces apoptosis, by modulating Bcl-xL and p53 both in murine aorta and in VSMCs. In addition, age-dependent increase in IL-6 and Prep1 in senescent VSMCs and in old mice may be involved in the aging-related vascular dysfunction.

KEYWORDS
aging, apoptosis, interleukin 6, Prep1, vascular smooth muscle cells

1 | INTRODUCTION

Apoptosis is a complex phenomenon regulated by many genes encoding for growth factors, cytokines, and transcription factors.[1,2] This process can be both physiological, as it occurs during embryogenesis and morphogenesis, and pathological since its dysregulation may cause several diseases. In particular, while reduced apoptosis has been associated with a higher risk of tumors and autoimmune diseases, in neurodegenerative diseases, such as Parkinson's or Alzheimer's diseases, apoptosis is thought to account for much of the cell death and the progressive loss of neurons.[3,4] Interestingly, apoptosis reduction in VSMCs located in the media layer of the aorta, together with an excessive proliferation, has been observed during the aging.[5–8] Indeed, with the age, VSMCs accumulate and, under the stimulation of different factors, such as cytokines, migrate to the intima, creating a neointima.[9] This process involves a reciprocal regulation between the vascular endothelial cells and the VSMCs, although the molecular mechanisms are still not clear.[10]

Prep1 is a transcription factor, belonging to the three-amino acid loop extension (TALE) homeodomain proteins, which is involved in ontogenesis, metabolism, and tumorigenesis. Furthermore, Prep1 inhibits apoptosis by stimulating Bcl-xL gene expression and by modulating p53.[11–13] Most of these results have been obtained "in vivo" by using both hypomorphic homozygous ($Prep1^{i/i}$) and heterozygous ($Prep1^{i/+}$) mouse models, expressing 3–7 and 55%–57% of the protein, respectively. $Prep1^{-/-}$ embryos tend to die during pregnancy and show generalized apoptosis and overall organ hypoplasia.[14] A small percentage that survives lives a normal length life but have a complex and contradictory phenotype. Indeed, although they feature a better peripheral glucose and lipid metabolism, these animals are smaller, have an impaired olfactory perception and may develop spontaneous tumors.[12,15–20] Very recently, we have demonstrated that $Prep1^{i/+}$ mice feature attenuated placental angiogenesis and vessel formation.[21] More detailed experiments performed in mouse aortic endothelial cells (MAECs) have indicated that Prep1 increases the expression of several proangiogenic factors, such as IL-6, which are also involved in neointimal formation during the aging. In the present work, we show that Prep1 mediates IL-6-antiapoptotic action on VSMCs through a mechanism involving both p53 and Bcl-xL and this effect is particularly clear in senescence.

2 | MATERIAL AND METHODS

2.1 | Materials

Media, sera, antibiotics for cell culture, and the Lipofectamine reagent were all from Invitrogen (Grand Island, NY, USA). Prep1 plasmid cDNA (pRc/CMV-Prep1) has been designed in the laboratory and produced by Invitrogen (Grand Island, NY). FITC-conjugated Annexin V was purchased from BioLegend (San Diego, CA, USA). Propidium Iodide (PI), Etoposide, and H_2O_2 were obtained from Sigma-Aldrich (Darmstadt, Germany). BH3I-1, Prep1 (Cat# sc-25282, RRID:AB_2164128), ERK1/2 (Cat# sc-514302, RRID:AB_2571739), Caspase 3 (Cat# sc-1224, RRID:AB_630985), Caspase 9 (Cat# sc-56076, RRID:AB_781847), Bcl-xl (Cat# sc-1041, RRID:AB_630916), Bcl-2 (Cat# sc-783, RRID:AB_2243455), and Vinculin (Cat# sc-73614, RRID:AB_1131294) antibodies were from Santa Cruz Biotechnology (Dallas, TX, USA). p-ERK1/2 (Thr202/Tyr204) (Cat# 9101, RRID:AB_331646) and p53 antibody (Cat# 2524, RRID:AB_331743) were purchased from Cell Signaling Technologies Inc (Danvers, MA, USA). Recombinant IL-6 was purchased from Cell Guidance Systems LLC (St. Louis, MA, USA). Protein electrophoresis and Real-time PCR reagents were from Bio-Rad (Richmond, VA, USA). Western blotting and ECL reagents were purchased from Amersham Biosciences (Arlington Heights, IL, USA).

2.2 | Animals

$Prep1$ targeted mice were generated by gene trapping by Lexikon Genetics, Inc, (The Woodlands, Texas). C57BL/6J $Prep1^{i/+}$ mice ($Prep1^{i/+}$) and C57BL/6J wildtype (WT) littermates were housed two to three per cage at constant temperature and relative humidity and were acclimated to a 12-h light/dark cycle and had ad libitum access to food and water. Their general phenotype has been previously described.[16] All animal handling was approved by the Ethics Committee on Animal Use of University of Naples "Federico II" (permission number 176/2020-PR, prot. 39F3A.60) and complies with the standards of the European Union. 6- and 18-month-old male and female WT and $Prep1^{i/+}$ mice have been euthanized and aorta extracted for subsequent uses.

2.3 | Immunohistochemical procedures

Transversal sections at 3 μm were deparaffined in xylene and rehydrated in the decreasing series of alcohol. Peroxidases were blocked with a solution of hydrogen peroxide and methanol (4:1) for 15 min. Antigen retrieval pretreatments were performed using a HIER citrate buffer pH 6.0 (Bio-Optica, Milan, Italy) for 20 min at 98°C. Subsequently, the antibodies with rabbit host and mouse host followed two different protocols. For antibodies with rabbit host, immunohistochemistry was performed with

MACH1 Universal HRP-Polymer Detection Kit (Bio-Optica, Milan, Italy) according to the manufacturer protocol.[22] As primary antibodies were used: Polyclonal Rabbit Anti-Casp3 (Cat# ab4051, RRID:AB_304243, Abcam, United Kingdom) at 1:200 in PBS, Polyclonal Rabbit Anti-Casp9 (Cat# LS-C148247, RRID:AB_11130565, Lifespan Biosciences, USA) at 1:600 in PBS, Polyclonal Rabbit Anti-Bcl-x$_{S/L}$ (Cat# sc-1041, RRID:AB_630916, Santa Cruz Biotechnology, USA) at 1:200 in PBS and rabbit monoclonal antibody Anti-ki67 (Cat# clone SP6, RRID:AB_2721189, BioCare Medical, USA) at 1:50 in PBS. For the antibody with mouse host, immunohistochemistry was performed with MOM Kit (Vector Laboratories, Burlingame, CA, USA) according to the manufacturer protocol.[23] Mouse monoclonal antibody Anti-p53 (Cat# clone 1C12, RRID: AB_331743, Cell Signaling Technology, USA) was used as primary antibody at a dilution of 1:50 in PBS. DAB stain was quantified with Fiji (ImageJ, National Institutes of Health). For each case, three random 40× fields of the transverse section of the aorta were photographed under an optical microscope (Nikon E600; Nikon, Tokyo, Japan) associated with a digital camera (Nikon digital camera DMX1200).

For the markers with cytoplasmic expression (Caspase 3, Caspase 9, and Bcl-xL), the optical density was measured. The function "Color threshold" was used on each row image to measure the total area of the analyzed tissue (Hue 0-255, Saturation 0-255, Brightness 0-230). To evaluate the positive area, each raw image was processed with the Color Deconvolution function using the preset Hematoxylin + DAB settings. The mean gray value of the tunica media was measured, and a mean value for the three selected fields has been calculated for each case. The optical density (OD) has been calculated with the following formula: OD = log (max intensity/mean intensity), where max intensity = 255 for 8-bit images.[24]

For the markers with nucleic expression (ki67 and p53) the percentage of positive nuclei was evaluated. After processing row images with Color Deconvolution and threshold as above described, positive cells were counted with the Automatic Particle counting function with the following settings: range of area between 50 and 150 μm^2 and a range of circularity between 0.3 and 1.[23] The total number of positive cells for each case was expressed as the percentage of positive nuclei.

Double staining of TUNEL and the SMA was performed to discern apoptotic smooth muscle cell of the tunica media of the aorta. Briefly, 4-μm thick aorta sections were stained with the anti-SMA antibody (Cat# clone 1A4, RRID:AB_2223500, Dako, Denmark) at 1:200 in PBS and then the Alexa Fluor 488-conjugated F(ab')2-Goat anti-Mouse IgG (Cat# A-10684, RRID:AB_2534064, Thermo Fisher Scientific, Massachusetts, USA) at 1:200

in PBS.[25] The sections were then subjected to staining with the TUNEL Assay Kit-BrdU-Red (ab66110, Abcam, United Kingdom) following the manufacturer's manual.[26]

2.4 | Cell culture procedures and transfection

Rat aortic vascular smooth muscle cells (VSMCs) were a kind gift from Prof. G. Iaccarino, "Federico II" University of Naples. Cells were grown in DMEM containing 4.5 g/L glucose supplemented with 10% Fetal Bovine Serum (FBS), 2 mmol/L L-glutamine, 0.1 mmol/L non-essential amino acids, and 1% penicillin/streptomycin solution at 37°C in a humidified 95% air and 5% CO_2 atmosphere (all vol./vol.). Transient transfection of Prep1 plasmid cDNA (pRc/CMVPrep1) in VSMC cells was performed by the Lipofectamine reagent (Invitrogen) according to the manufacturer's instructions. For these studies, 60%–80% confluent cells were incubated for 8 h with 2 μg of plasmid construct and 6 μl of lipofectamine reagent and then were added DMEM 20% FBS. The day after, medium was replaced with DMEM with 10% FBS before being assayed.

2.5 | Peptide synthesis and characterization

The fragment of Prep1, spanning residues 54–72, conjugated to TAT at the C-terminus to facilitate cell uptake (hereafter called Prep (54–72); single letter sequence: Ac-KQAIYRHPLFPLLALLFEK-NH2-βA-TAT), was synthesized as acetylated and amidated derivative, purified and characterized as described previously.[27] Prep1 (54–72) peptide was used at 25 μM concentration for 18 h and vehiculated by the Lipofectamine reagent (Invitrogen) into cells. As control, VSMCs were incubated with a non-specific peptide (NC).[20,21,28] Sulforhodamine B assay was performed as described by Ricci S et al.[19]

2.6 | Western blot analysis

Total cell lysates were obtained and separated by SDS-PAGE. Briefly, tissue samples were homogenized in a Polytron (Brinkman Instruments, NY) in 10 ml T-PER reagent/g of tissue according to the manufacturer (Pierce, IL). After centrifugation at 10,000 rpm for 5 min, the supernatant was collected. Cells were solubilized with lysis buffer containing 50 mM HEPES, 150 mM NaCl, 10 mM EDTA, 10 mM $Na_4P_2O_7$, 2 mM sodium orthovanadate, 50 mM NaF, 1 mM phenylmethylsulfonyl fluoride, 10 μg/ml aprotinin, 10 μg/ml leupeptin, pH 7.4, and 1% (v/v)

Triton X-100. Lysates were clarified by centrifugation at 14,000 rpm for 20 min at 4°C. Protein concentrations in the cell lysates were measured using a Bio-Rad DC (detergent compatible) assay. Western blot analysis has been performed as previously described.[29,30]

2.7 | Real-time RT-PCR analysis

Total cellular RNA was isolated from mice aorta and VSMC cells by using the RNeasy kit (QIAGEN Sciences, Germany), according to manufacturer instructions. 1 μg of cell RNA was reverse-transcribed using Superscript III Reverse Transcriptase (Life Technologies Carlsbad, CA, USA). PCR reactions were analyzed using IQTM SYBR Green Supermix (Bio-Rad, Hercules, CA). Reactions were performed using Platinum SYBR Green qPCR Super-UDG using an iCycler IQ multicolor Real Time PCR Detection System (Biorad, CA). All reactions were performed in triplicate and β-actin was used as an internal standard. Relative quantification of gene expression was measured by using $2^{-\Delta\Delta Ct}$ method.[31] Primer sequences used are described in Table 1.

2.8 | Annexin V/PI staining

VSMC cells were collected and washed with Annexin V binding buffer (BioLegend, San Diego, CA, USA). Pellet was resuspended in Annexin V binding buffer containing FITC-conjugated Annexin V. After 15′ incubation at room temperature, Propidium Iodide (PI) solution (0.015 M

in PBS) was added to each sample just before analysis. All samples were acquired with a BD LSRFortessa (BD Biosciences, San Jose, CA, USA) and analyzed using the BD FACSDiva Software.

2.9 | Statistical procedures

Data were analyzed with GraphPad Prism 7.0 (GraphPad Inc, San Diego, CA, USA) by unpaired two-tailed Student's t-test. p values equal or less than .05 were considered statistically significant.

3 | RESULTS

3.1 | Aortic Prep1 deficiency reduces medial smooth muscle density by increasing apoptotic pathway

We first evaluated the levels of Prep1 in aorta of WT and $Prep1^{i/+}$ mice. Immunohistochemistry showed a stronger immunoreaction of endothelial cells (EC), tunica media (TM) and tunica adventitia (TA) to Prep1 antibody in WT mice compared to $Prep1^{i/+}$ littermates (Figure 1A). Interestingly, Prep1 deficiency decreased medial smooth muscle cell (SMC) density by 25% (Figure 1B). In order to understand the mechanisms by which Prep1 could affect the number of SMC, sections from WT and $Prep1^{i/+}$ mice were stained with ki67 antibody to evaluate proliferation. As shown in Figure 1C, the number of ki67-positive nuclei was similar in WT and $Prep1^{i/+}$ mice. However,

TABLE 1 Primer sequences used in real-time RT-PCR analysis

| Primer	Forward (5′-3′)	Reverse (3′-5′)
Prep1	CCTGGGACAATTAGGATCCAGAACT	TCCTCTGTTGGGTAGGGATGCC
Caspase 3	TGGAGAACAACAAAACCTCAGTG	TCCAGATAGATCCCAGAGTCCA
Caspase 9	TGTTCTTCATCCAGGCCTGT	CTGGGAAGGTGGAGTAGGAC
Bcl-xL	GACCGCGTATCAGAGCTTTG	GTTCTCCTGGATCCAAGGCT
p53	GCTCCTCTCCCCAGCAAAAG	GCTCACGCCCACGGATTAAG
p16^INK4	CTTCTGCTCAACTACGGTGC	GCACGATGTCTTGATGTCCC
p21^Waf1	CAAAGTGTGCCGTTGTCTCT	AGGAAGTACTGGGCCTCTTG
IL6	GCCAGAGTCCTTCAGAGAGA	GGTCTTGGTCCTTAGCCACT
bFGF	CTTCTTCCTGCGCATCCATC	AGCCGTCCATCTTCCTTCAT
VEGF-A	TTGTTCAGAGCGGAGAAAGC	TTTAACTCAAGCTGCCTCGC
TGFβ	GCCAGAGTCCTTCAGAGAGA	GGTCTTGGTCCTTAGCCACT
IL8	AGCCACCCGCTCGCTTCTCT	TCGGTTTGGGTGCAGTGGGG
CCL5	ACACCACTCCCTGCTGCTTT	TTCTGTGGGTTGGCACACAC
GLB1	TGCAGCTGTGGATAAATGGC	CAGGGTCCCACACTTGAGTA
b-Actin	GGTGGGAATGGGTCAGAAGG	GTTGGCCTTAGGGTTCAGGG
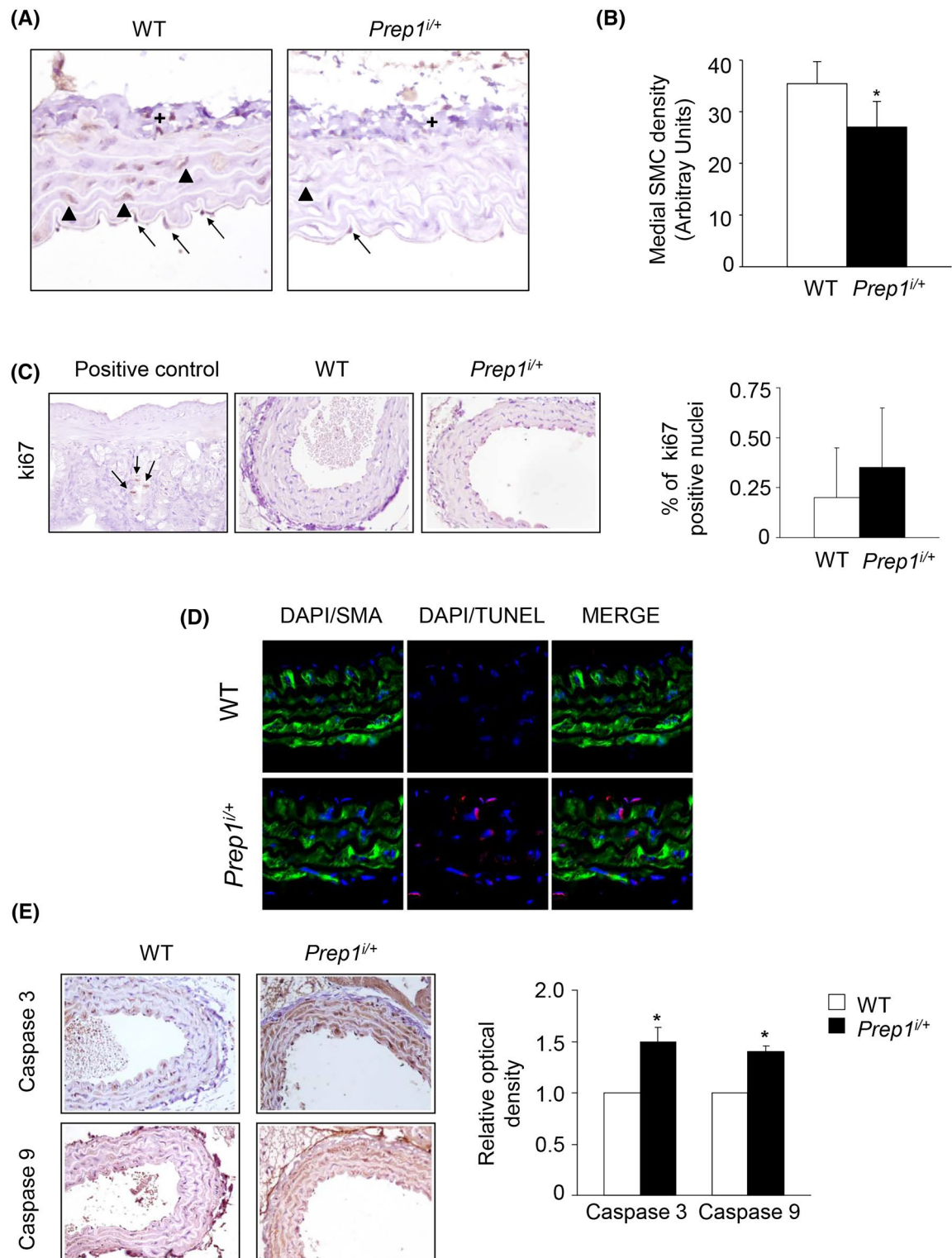
FIGURE 1 Morphological evaluation of thoracic aorta in wild type and *Prep1*[i/+] mice. (A) Immunohistochemical staining of WT and *Prep1*[i/+] thoracic aortas for Prep1 (40× original magnification). A nuclear immunopositivity for Prep1 antibody is evident in tunica intima (arrows), tunica media (arrowheads) and tunica adventitia (+) of WT mice compared to *Prep1*[i/+] littermates. (B) Bar graph of the medial smooth muscle density. (C) Intestinal crypt from a WT mouse, positive control for Ki67 (arrows, 40× original magnification). Representative immunohistochemical staining for ki67 from 6-month-old WT and *Prep1*[i/+] mice (40× magnification) and corresponding bar graph of the quantitative assessment of the immunolabeling. (D) Representative double staining of WT and *Prep1*[i/+] thoracic aortas for TUNEL and SMA (40× original magnification). (E) Representative immunohistochemical staining for Caspase3 and Caspase 9 from 6-month-old WT and *Prep1*[i/+] mice (40X magnification) and corresponding bar graph of the quantitative assessment of the immunolabeling. Values are mean ± SD of six mice for groups. Asterisks denote statistical differences (*$p < .05$)
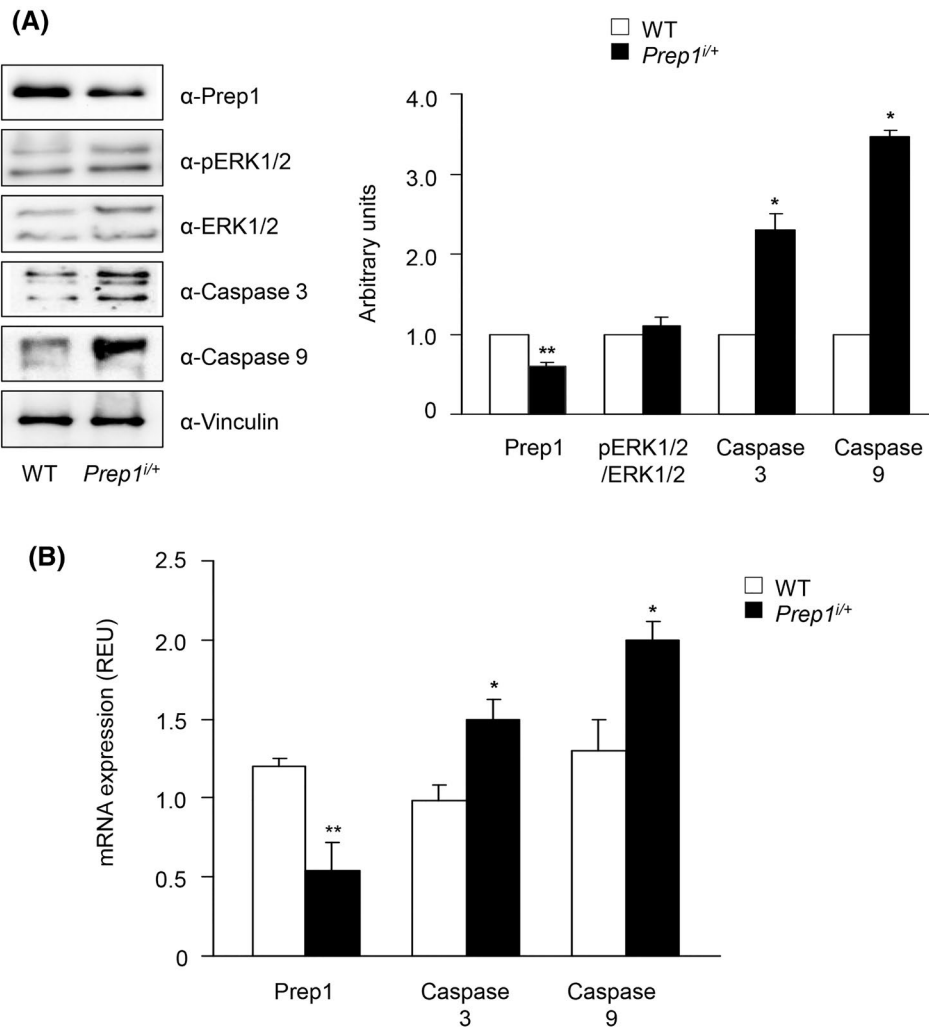
FIGURE 2 Evaluation of protein and mRNA levels of Prep1, caspase 3 and 9 in WT and *Prep1*[i/+] mice. (A) Aortas from 6-month-old WT and *Prep1*[i/+] mice were solubilized and protein samples analyzed by Western Blot with Prep1, Caspase3, Caspase 9 antibodies. Vinculin antibody was used for normalization. Blot were revealed by ECL, and autoradiograph is representative of three independent experiments and subjected to densitometric analysis. (B) *Prep1*, *Caspase3*, *Caspase 9* mRNAs were determined by Real-time RT-PCR analysis of total RNA isolated from the aorta of 6-month-old WT and *Prep1*[i/+] mice, using *β-actin* as internal standard. Bar represents the mean ± SD of three independent experiments, in each of which reactions were performed in triplicate using total RNAs obtained from six mice per genotype. Asterisks denote statistical differences (*$p < .05$; **$p < .01$)

TUNEL-SMC double staining indicated that the number of apoptotic cells was significantly higher in *Prep1*[i/+] animals compared to the WT littermates and this result was paralleled by a 1.5-fold increase in caspase 3 and 9, suggesting a larger spontaneous apoptosis (Figure 1D,E). To confirm these data, we measured the levels of Prep1, ERK1/2 and caspases in the aortic lysates. *Prep1*[i/+] mice displayed a 40% reduction in Prep1 protein levels compared to the WT littermates, while both total and phosphorylated amount of ERK1/2 did not change. However, caspase 3 and 9 increased by 2.3- and 3.5-fold in Prep1 deficient mice, respectively (Figure 2A). In parallel, mRNA levels of Prep1 were 50% decreased, unlike caspases that were significantly higher in *Prep1*[i/+] mice than in WT

animals (Figure 2B). Next, we measured the levels of Bcl-xL and p53, previously described to be regulated by Prep1 (11–13). Immunostaining experiments revealed reduction in Bcl-xL (although not statistically significant), while p53 was significantly upregulated by 2.8-fold in media layer between WT and *Prep1*[i/+] mice (Figure 3A). Total aortic Bcl-xL and p53 protein levels were 40% lower and 3-fold higher in *Prep1*[i/+] mice than in WT littermates, respectively. Bcl-2, another important antiapoptotic protein which is not directly regulated by Prep1, did not change between the WT and *Prep1*[i/+] animals (Figure 3B). In parallel, *Prep1*[i/+] mice showed a 30% reduction in Bcl-xL mRNA levels with a significant increase in p53 expression compared to the control littermates (Figure 3C).
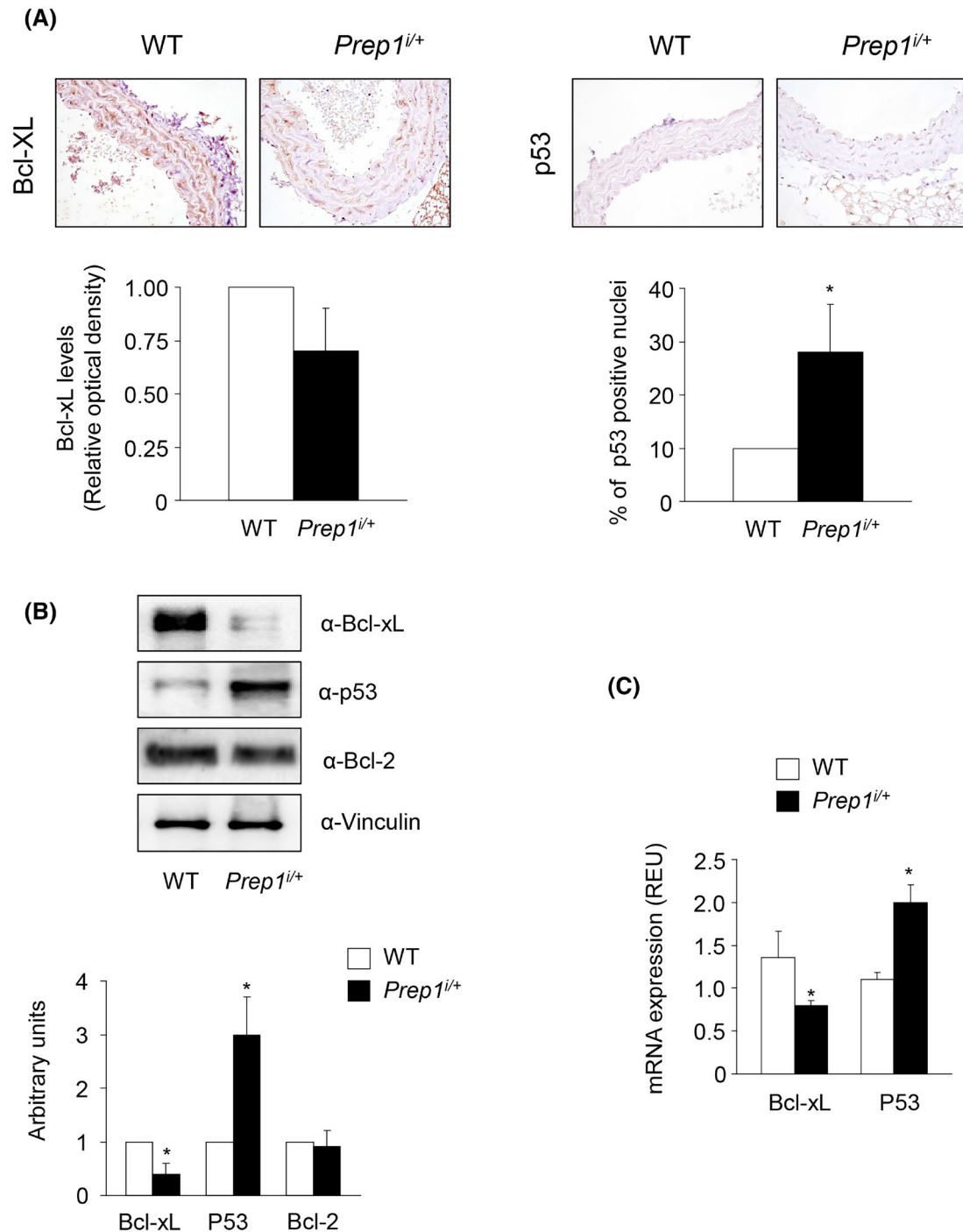
FIGURE 3 Immunohistochemical expression of Bcl-xL and p53 in WT and *Prep1*[i/+] mice. (A) Immunohistochemical staining of 6-month-old WT and *Prep1*[i/+] thoracic aortas for Bcl-xL and p53 (40× magnification) and corresponding bar graph of the quantitative assessment of the immunolabeling. Values are mean ± SD of six mice for groups. (B) Protein samples were obtained from aortas of 6-month-old WT and *Prep1*[i/+] mice. Protein expression of Bcl-xL, p53 and Bcl-2 were analyzed by Western Blot using vinculin antibody for normalization. Blot were revealed by ECL, and autoradiograph is representative of three independent experiments and subjected to densitometric analysis. (C) mRNA abundance of *Bcl-xL* and *p53* was measured by Real-time RT-PCR analysis of total RNA isolated from aorta of 6-month-old *Prep1*[i/+] and control mice, using *beta-actin* as internal standard. Bar represents the mean ± SD of three independent experiments, in each of which reactions were performed in triplicate using total RNAs obtained from six mice per genotype. Asterisks denote statistical differences (*$p < .05$)

3.2 | Prep1 regulates VSMCs apoptosis

To further address the mechanism by which Prep1 could regulate the SMC density, we transiently transfected VSMCs with an empty vector (CTRL) or with Prep1 cDNA (*Prep1*). The measure of Prep1 protein and mRNA levels indicated a 3- and 6-fold increase in Prep1 protein amount and transcript, respectively (Figure 4A,B). Flow cytometry using Annexin V/PI binding indicated 25% reduced apoptosis in *Prep1* VSMCs compared to the control cells (Figure 4C). This result was consistent with a 40, 37, and 50% reduction in caspase 3, caspase 9 and p53 protein levels, respectively, in Prep1 overexpressing cells. In contrast, Bcl-xL was induced by 1.3-fold in presence of Prep1 (Figure 4D). Next, we investigated the specific role of Bcl-xL and p53 in Prep1-mediated apoptosis. To this end, we incubated CTRL and Prep1 overexpressing VSMCs with a Bcl-xL specific inhibitor, BH3I-1, or with etoposide, a p53 activator. As shown in Figure 5A, Prep1 induced Bcl-xL expression by 1.2-fold and reduced caspase 3 and 9 expression by 30%. Interestingly, treatment with BH3I-1 reverted the effect of Prep1 on the apoptotic mediators. In parallel, Prep1 reduced p53, caspase 3 and 9 transcripts by 30%, 45% and 50%, and administration of etoposide rescued this event (Figure 5B). We next measured DNA damage by evaluating the presence of histone H2AX (γ-H2AX). Prep1 reduced the percent of γ-H2AX positive cells by 23% compared to the control VSMCs (Figure S1).

3.3 | Aging increases Prep1 levels in aorta and in VSMCs

Several authors have shown that aging-associated excessive neointimal formation may be due in part to a reduction in VSMCs apoptosis.[6,10,32] To evaluate a possible role of Prep1 in the aging, we first measured the levels of Prep1 and two senescence markers, p16[INK4] and p21[Waf1]. Real-time RT-PCR experiments performed in 6- and 18-month-old WT mice indicated that expression of Prep1, p16[INK4] and p21[Waf1] increased by 90%, 30% and 90% in the aorta of aged mice compared to the youngest animals (Figure 6A). Aging markers were comparable between WT and *Prep1*[i/+] mice. Indeed, despite of 55 and 58% lower Prep1 levels in *Prep1*[i/+] mice at 6 and 18 months than the WT littermates, p16[INK4] and p21[Waf1] increased by 90% and 50% in old Prep1 deficient mice (Figure S2).

In parallel, IL-6 levels and CCL-5 were 2.2- and 1.2-fold induced by the aging, respectively, while other molecules, such as FGF, VEGF, TGFβ and IL-8 did not significantly change (Figure 6B). To confirm the data obtained "in vivo", we induced VSMCs senescence by treating cells with 200 μM hydrogen peroxide (H_2O_2). This concentration was not toxic to the cells (data not shown), but increased β-galactosidase (GLB1) gene expression by 2-fold compared to the untreated VSMCs (Figure 6C). Like in mice, aged VSMCs featured increased levels of Prep1, p16[INK4] and p21[Waf1] and IL-6 by 110, 85, 70 and 135% compared to the untreated cells (Figure 6D).

3.4 | Prep1 mediates IL-6-induced apoptosis in senescent VSMCs

In order to investigate whether IL-6 could be upstream of Prep1 action on VSMCs, we stimulated young and senescent cells with IL-6. Real-time RT-PCR revealed a 3-fold increase in Prep1 expression after incubation with IL-6 in old cells, while in young VSMC the increase was less than 1-fold (Figure 7A). Caspase 3, caspase 9 and p53 showed a similar reduction in presence of IL-6 both in young and in senescent cells (Figure 7B–D). Similarly, Bcl-xL expression was almost 60% induced by IL-6 before and after treatment with H_2O_2 (Figure 7E). Interestingly, treatment of VSMCs with the synthetic Prep1 inhibitor peptide Prep1 (54–72) did not modify cell viability (Figure S3) and affect Prep1 expression (Figure 7A) but reverted the effects of IL-6 on apoptotic mediators, particularly in senescent cells. Indeed, in young cells, caspase 3, 9 and p53 levels were increased by 1.8, 2.2 and 1.8-fold in presence of IL-6 and Prep1 (54–72) compared to IL-6 alone, while in old VSMCs they were induced by 2.5, 2.9 and 2.4 (Figure 7B–D). Consistently, Bcl-xL expression was downregulated by 45% and 60% in young and senescent cells, respectively, after treatment with IL-6 and Prep1 (54–72) (Figure 7E).

4 | DISCUSSION

TALE (three amino acid loop extension) subclass of homeodomain proteins includes several transcription factors (TFs) involved in the ontogenesis. Among these TFs, Prep1, by interacting with different cofactors, plays a significant role in organs and tissues development, in tumorigenesis and in metabolism. In particular, Prep1 binding to Pbx1 regulates the expression of several genes, including HOX proteins, IL-3, stromelysin, urokinase plasminogen activator and follicle stimulating hormone beta subunit.[33–35] Interestingly, the same complex suppresses the glucagon promoter in non-glucagon-producing cells.[36] Prep1, in collaboration with another cofactor, p160, inhibits HoxB2 expression.[37] Other evidence indicates that Prep1 acts as a regulator of apoptosis. *Prep1*[i/i] mice show a marked and widespread apoptosis[14] and the function of Prep1 in the regulation

(A)

α-Prep1

α-Vinculin

(B)

(C)

(D)

α-Caspase 3

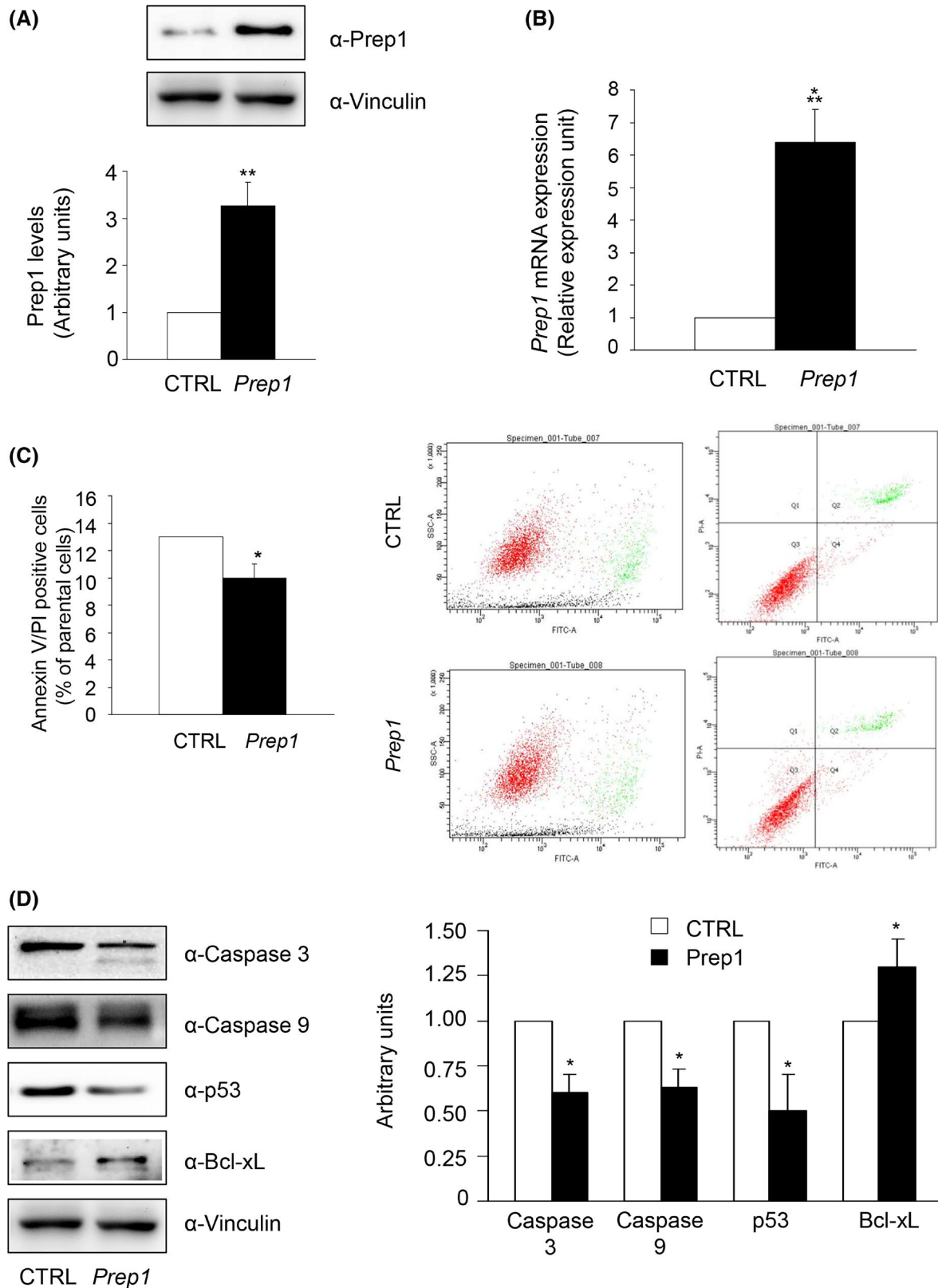α-Caspase 9

α-p53

α-Bcl-xL

α-Vinculin

CTRL   *Prep1*

FIGURE 4 Evaluation of apoptosis in control and in Prep1 overexpressing VSMCs. (A,D) VSMCs were transfected with *Prep1* cDNA (*Prep1*) and with empty vector (CTRL). Protein levels were analyzed by Western blot using antibodies for Prep1, Caspase 3, Caspase 9, Bcl-xL, p53 and Vinculin, which was used for normalization. The autoradiographs shown are representative of three different experiments and subjected to densitometric analysis. (B) *Prep1*mRNA levels were analyzed by Real-time RT-PCR analysis, using *beta-actin* as internal standard. Bars represent the mean ± SD of three independent experiments, each performed in triplicate. (C) Apoptotic cells were quantified using annexin V-FITC staining and FACS analysis. Numbers indicate the percentage of Annexin V-positive cells. Asterisks denote statistical differences (*$p < .05$; **$p < .01$; ***$p < .001$)
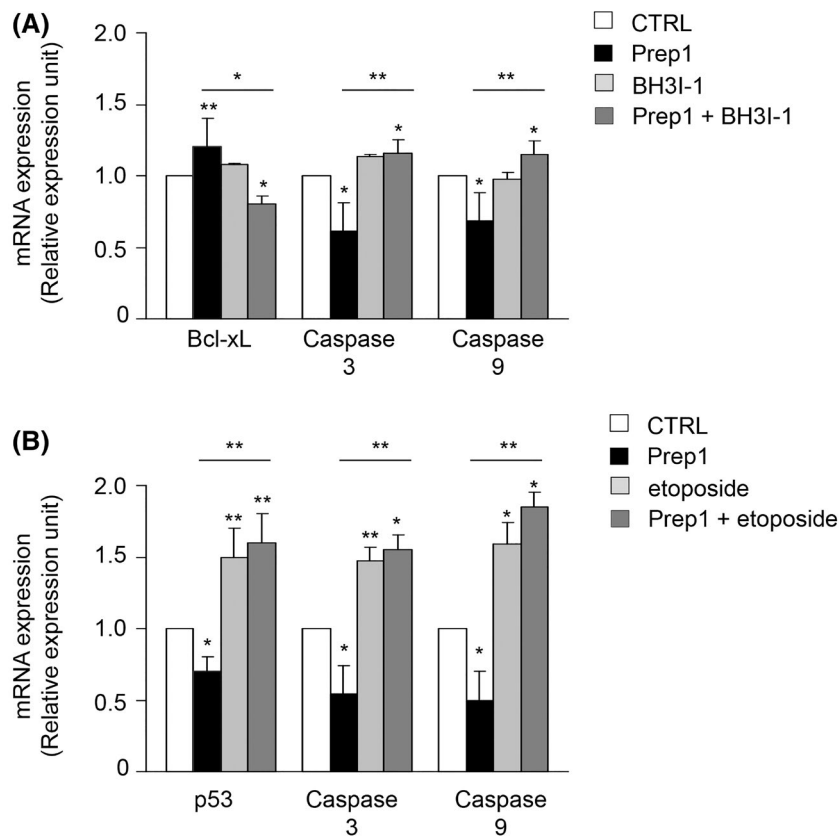
FIGURE 5 Inhibition of Bcl-xL and activation of p53 reverts the antiapoptotic effects of Prep1. (A) CTRL and *Prep1* VSMCs were treated with the Bcl-xL inhibitor BH3I-1 (25 μM) for 24 h. *Bcl-xL*, *Caspase3*, *Caspase 9* mRNAs were determined by Real-time RT-PCR analysis of total RNA, using β-actin as internal standard. Bars represent the mean ± SD of three independent experiments, each performed in triplicate. (B) CTRL and *Prep1* VSMCs were treated with the p53 activator etoposide (20 μM) for 24 h. *p53*, *Caspase3*, *Caspase 9* mRNAs were determined by Real-time RT-PCR analysis of total RNA, using *β-actin* as internal standard. Bars represent the mean ± SD of three independent experiments, each performed in triplicate. Asterisks denote statistical differences (*$p < .05$; **$p < .01$)

of cell death is mediated by the anti-apoptotic protein Bcl-xL or by the pro-apoptotic p53. Indeed, chromatin immunoprecipitation (ChIP) assays of the *Bcl-x* promoter suggest that Bcl-xL is transcriptionally upregulated by Prep1, and its levels are reduced in mouse embryo fibroblasts (MEF) and fetal liver cells of *Prep1*[i/i] mice.[11,13] The action of Prep1 on p53 is not very clear. Prep1 overexpression in F9 teratocarcinoma cells or in *Prep1*[i/i] MEF increases the expression of p53 as indicated by ChIP experiments,[13] while, in contrast, the absence of Prep1 causes p53-dependent apoptosis of epiblast cells.[12] It is difficult to explain this discrepancy, however, we may suppose that it depends on the different cell types or the specific Prep1 cofactors.

Apoptotic processes are involved in the development of the organisms, in the formation and regulation of the immune system and in the elimination of potentially defective and harmful cells. Dysfunctions of the apoptotic program can cause tumors, autoimmune diseases, and the spread of viral diseases, while excesses of apoptosis have often been associated with neurodegenerative and ischemic diseases, particularly during aging.[3]

Our recent studies performed in *Prep1*[i/+] mice and in MAECs revealed that Prep1 stimulates the formation of new blood vessels, by increasing angiogenic molecules, some of which are also involved in vascular dysfunction during the aging.[21]

In the current work we have investigated the role of Prep1 in the medial muscle component of the aorta and in VSMCs and, its possible correlation with aging.

Aortas from *Prep1*[i/+] mice display medial smooth muscle cell density reduction, which is paralleled by a significant increase in apoptosis and caspase 3 and 9 levels. Ki67, a marker of cell proliferation, show no difference between WT and *Prep1*[i/+] mice and this data, confirmed also by measuring ERK1/2 phosphorylation in total aorta lysates, is consistent with those reported by Fernandez-Diaz et al in *Prep1*[i/i] and *Prep1*[i/+] embryos.[12] Furthermore, our observations suggest a role of Prep1 on apoptosis not only in embryos, but also in adult mice. The increased levels of caspases in *Prep1*[i/+] aortic tunica media, also confirmed in total aortic homogenates, are due to the upregulation of p53 and the reduction in Bcl-xL, which have previously been described to be modulated by Prep1 (11–13). Indeed, Bcl-xL tended to be downregulated, while p53 was strongly induced in media layer of *Prep1*[i/+] mice compared to the WT animals. These differences were also evident in aortic total lysates. Unlike Bcl-xL and p53, Bcl-2, another apoptosis suppressor gene which is not directly regulated by Prep1, did not change between WT and *Prep1*[i/+] animals.

To support the observations obtained "in vivo", VSMCs have been transfected with *Prep1* cDNA (*Prep1*). Prep1 overexpression attenuates apoptosis mediated by caspases 3 and 9, and, interestingly, both inhibition of Bcl-xL or activation
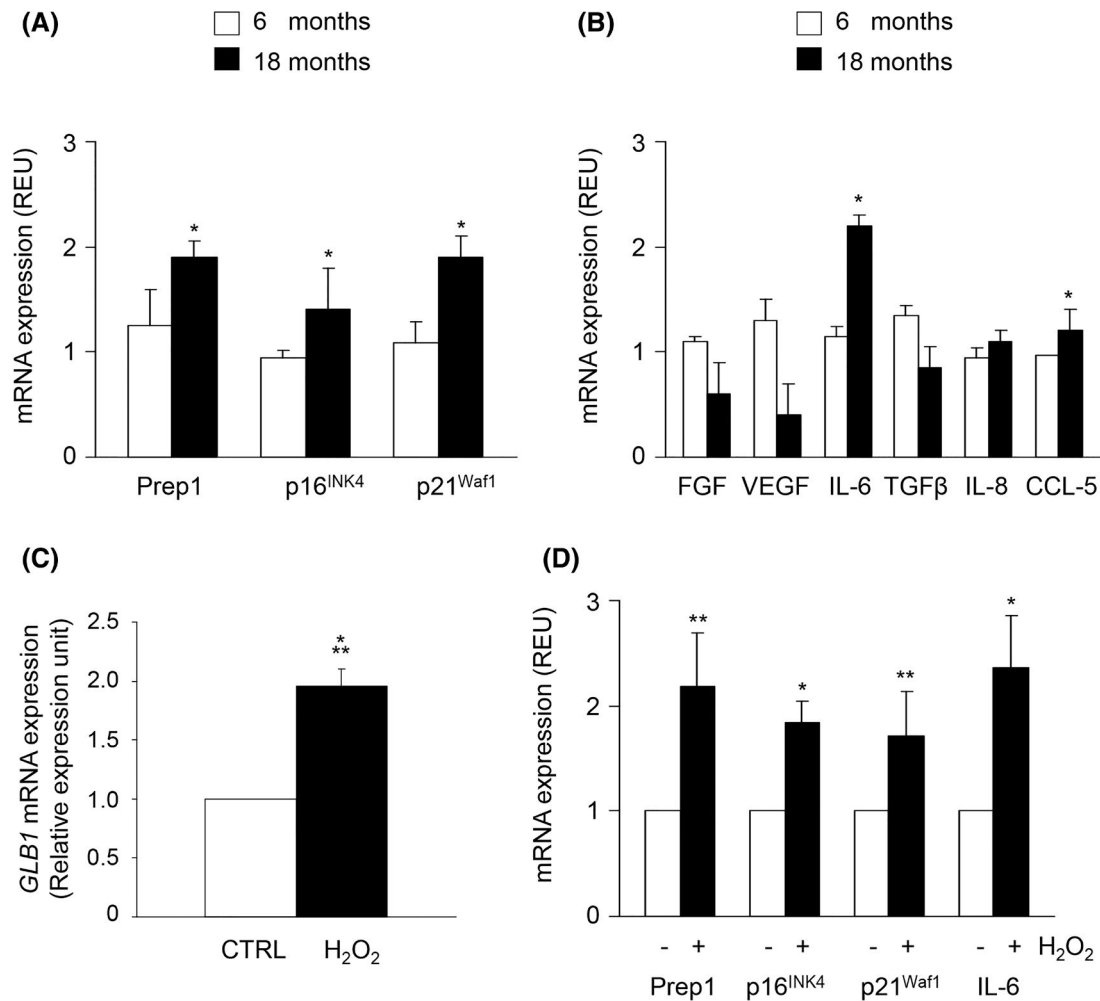
FIGURE 6 Role of Prep1 in the aging. (A,B) *Prep1*, *p16^INK4* and *p21^Waf1* and *FGF*, *VEGF*, *IL-6*, *TGFβ*, *IL-8* and *CCL-5* mRNAs were determined by Real-time RT-PCR analysis of total RNA isolated from the aorta of 6- and 18-month-old WT mice, using *β-actin* as internal standard. Bar represents the mean ± SD of three independent experiments, in each of which reactions were performed in triplicate. (C) *GLB1* mRNA expression was evaluated as described above, using *β-actin* as internal standard. (D) CTRL and *Prep1* VSMCs were treated with H_2O_2 at 200 µM concentration for 24 h and *Prep1*, *p16^INK4* and *p21^Waf1* and *IL-6* mRNA levels were evaluated as described above, using *β-actin* as internal standard. Bars represent the mean ± SD of three independent experiments, each performed in triplicate. Asterisks denote statistical differences (*$p < .05$; **$p < .01$)

of p53 revert the antiapoptotic effect of Prep1. In a manuscript by Fernandez-Diaz et al, the authors suppose that Prep1 deficiency may cause DNA damage leading to p53-induced apoptosis of epiblast cells.[12] Interestingly, γ-H2AX, a DNA damage marker, was lower in VSMCs overexpressing Prep1 than control cells, supporting their hypothesis.

Aging is an important risk factor of several cardiovascular diseases as it stimulates neointimal formation.[32] During the aging, blood vessel wall broadens and develops a thickened intima as consequence of increased proliferation and reduced susceptibility to apoptosis of VSMCs. Furthermore, inflammatory cells infiltrating intima induce local inflammation.[6,10,32,38,39] Although exaggerated neointimal formation in aging humans and animals is well documented,[6] the mechanisms responsible for this process are not clearly understood.

In order to assess a possible pathophysiological role of Prep1-regulated apoptosis, we have evaluated the aortic levels of Prep1 and two senescence markers, p16^INK4 and p21^Waf1, in the aging (18 months) and adult (6 months) WT mice. Both proteins were upregulated in old WT mice and a similar trend was also observed in *Prep1^i/+* mice. In parallel, IL-6 particularly increases in the 18 months WT mice. Comparable results have also been detected by treating VSMCs with hydrogen peroxide (H_2O_2), a reagent widely used to induce premature senescence within a short period of time.[40]

The role of IL-6 in aging and in vascular dysfunction has been well described. Indeed, increased serum concentration of IL-6 with age has been related to the physical function decline and chronic diseases which often affect older persons.[41–48] In addition, Wang
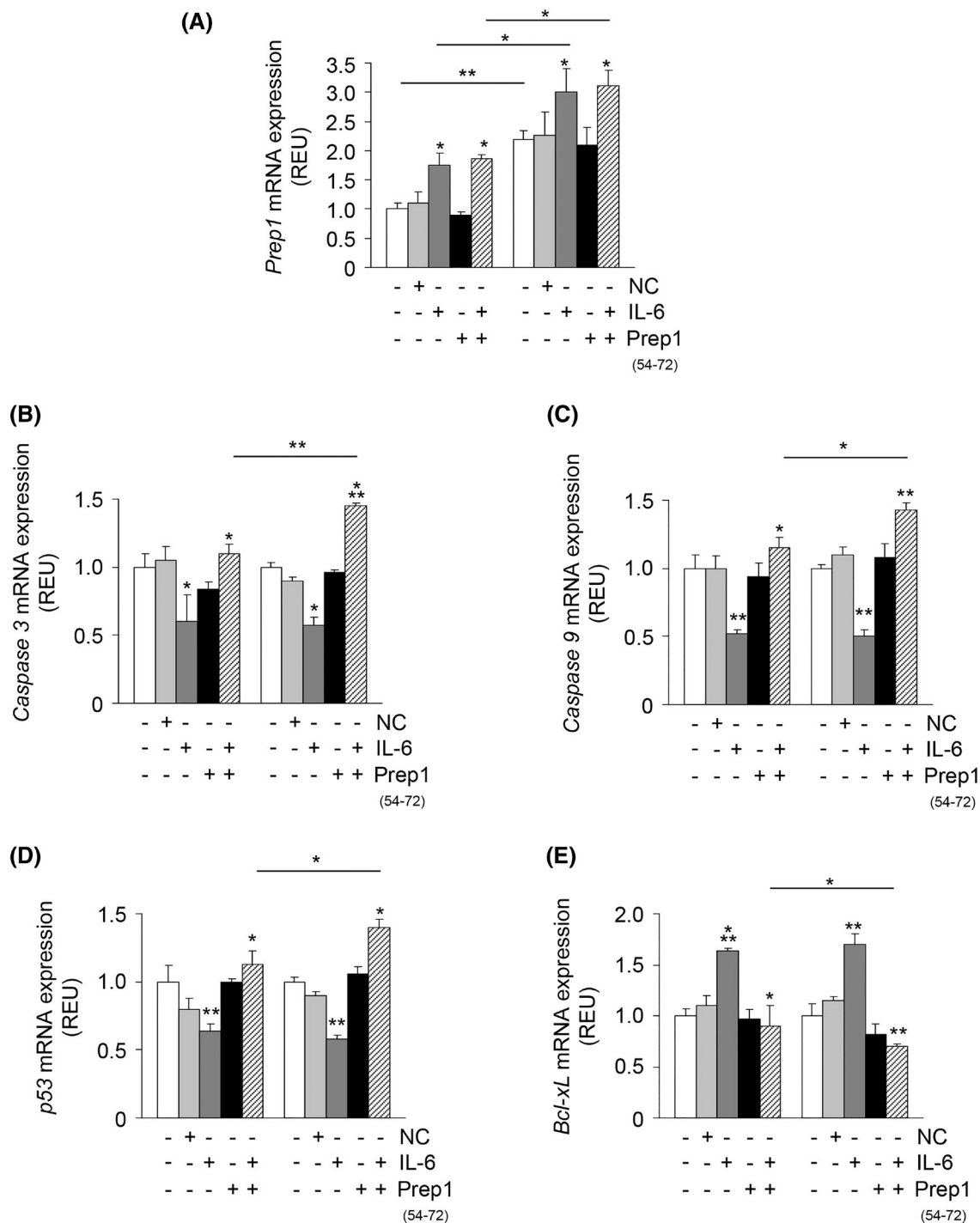
FIGURE 7 Prep1 inhibition reverts the antiapoptotic effects of IL-6 in senescent VSMCs. Cellular senescence was induced by treating VSMCs with H_2O_2 (200 μM) for 24 h. Both young and old cells were in presence of only medium (white bars) or incubated with non-specific peptide (NC) (light gray bars), IL-6 (10 ng/ml) (dark gray bars), *Prep1* cDNA (black bars) and Prep1 (54–72) (bars with oblique lines). *Prep1* (A), *Caspase 3* (B), *Caspase 9* (C), *p53* (D) and *Bcl-xL* (E) were determined by Real-time RT-PCR analysis using *β-actin* as internal standard. Bars represent the mean ± SD of three independent experiments, each performed in triplicate. Asterisks denote statistical differences (*$p < .05$; **$p < .01$; ***$p < .001$)

et al have demonstrated that IL-6, which is elevated in the arterial wall in atherosclerosis and restenosis after angioplasty, stimulates migration of VSMCs from the media to the intima.[9] Based on these observations and on the antiapoptotic role of IL-6 in different tissues,[49,50]

we have evaluated the possibility that IL-6 may be upstream of the Prep1-regulated apoptotic signaling in the senescent VSMCs. IL-6 increases Prep1 expression more in the aged that in young VSMCs, while no significant differences have been observed in caspase 3,

caspase 9, p53 and Bcl-xL levels between young and senescent cells.

The presence of the previously described Prep1 synthetic peptide, Prep1 (54–72),[20,21,28] which, by preventing the binding of Prep1 with p160, inhibits the action of Prep1, reduced the antiapoptotic effects mediated by IL-6 much more effectively in senescent than in young VSMCs, corroborating our hypothesis. Nevertheless, further studies, currently underway in our laboratory, are needed to evaluate the role of the Prep1 binding partners on the age-induced VSMCs apoptosis.

Similarly, the possible mechanism through which IL-6 acts on Prep1 is unclear. IL-6 activates intracellular signaling pathways though its membrane-bound receptor (IL-6R), which is present on few cells in the body (classic signaling). However, IL-6 can also bind to soluble forms of the IL-6R (sIL-6R) and induce effects in other cell types (trans-signaling). Klouche et al indicate that human primary smooth muscle cells responded only marginally to IL-6 but better in presence of IL-6 and sIL-6R.[51] Our experiments have been performed in rodent VSMCs which are responsive to IL-6 as evidenced by several authors.[9,52–54] Thus, whether sIL-6R may improve IL-6 signaling also in our cellular model remains to be clarified.

In conclusions, the present study provides new knowledge of the homeodomain transcription factor Prep1 on the age-induced VSMCs apoptosis, leading to hypothesize Prep1 as new possible target for the prevention of vascular alterations in aging individuals.

DISCLOSURES
There are no conflicts of interest to declare.

AUTHOR CONTRIBUTIONS
Ilaria Cimmino designed, performed the research, and analyzed the data. Francesco Prisco, Sonia Orso, Ayewa L. Agognon, Pasquale Liguoro, Davide De Biase, Orlando Paciello performed the research. Nunzianna Doti and Menotti Ruvo contributed with specific reagents. Francesco Beguinot and Pietro Formisano designed the research and analyzed the data. Francesco Oriente designed the research, analyzed the data, and wrote the paper. All the authors critically revised the article and approved the final version.

ORCID
Pietro Formisano https://orcid.org/0000-0001-7020-6870
Francesco Oriente https://orcid.org/0000-0003-4375-4526

REFERENCES
1. Wang E, Marcotte R, Petroulakis E. Signaling pathway for apoptosis: a racetrack for life or death. *J Cell Biochem*. 1999;75(suppl 32):95-102.
2. Lavrik IN. Systems biology of apoptosis signaling networks. *Curr Opin Biotechnol*. 2010;21(4):551-555.
3. Favaloro B, Allocati N, Graziano V, et al. Role of apoptosis in disease. *Aging*. 2012;4(5):330-349.
4. Rudin CM, Thompson CB. Apoptosis and disease: regulation and clinical relevance of programmed cell death. *Annu Rev Med*. 1997;48:267-281.
5. Uryga AK, Bennett MR. Ageing induced vascular smooth muscle cell senescence in atherosclerosis. *J Physiol*. 2016;594(8):2115-2124.
6. Tower J. Programmed cell death in aging. *Ageing Res Rev*. 2015;23(Pt A):90-100.
7. Rodriguez-Menocal L, Faridi MH, Martinez L, et al. Macrophage-derived IL-18 and increased fibrinogen deposition are age-related inflammatory signatures of vascular remodeling. *Am J Physiol Heart Circ Physiol*. 2014;306(5):H641-H653.
8. Wang JC, Bennett M. Aging and atherosclerosis: mechanisms, functional consequences, and potential therapeutics for cellular senescence. *Circ Res*. 2012;111(2):245-259.
9. Wang Z, Newman WH. Smooth muscle cell migration stimulated by interleukin 6 is associated with cytoskeletal reorganization. *J Surg Res*. 2003;111(2):261-266.
10. Qian D, Wu X, Jiang H, et al. Aging reduces susceptibility of vascular smooth muscle cells to H(2)O(2)-induced apoptosis through the down-regulation of Jagged1 expression in endothelial cells. *Int J Mol Med*. 2011;28(2):207-213.
11. Micali N, Ferrai C, Fernandez-Diaz LC, et al. Prep1 directly regulates the intrinsic apoptotic pathway by controlling Bcl-XL levels. *Mol Cell Biol*. 2009;29(5):1143-1151.
12. Fernandez-Diaz LC, Laurent A, Girasoli S, et al. The absence of Prep1 causes p53-dependent apoptosis of mouse pluripotent epiblast cells. *Development*. 2010;137(20):3393-3403.
13. Micali N, Longobardi E, Iotti G, et al. Down syndrome fibroblasts and mouse Prep1-overexpressing cells display increased sensitivity to genotoxic stress. *Nucleic Acids Res*. 2010;38(11):3595-3604.
14. Ferretti E, Villaescusa JC, Di Rosa P, et al. Hypomorphic mutation of the TALE gene Prep1 (pKnox1) causes a major reduction of Pbx and Meis proteins and a pleiotropic embryonic phenotype. *Mol Cell Biol*. 2006;26(15):5650-5662.
15. Longobardi E, Iotti G, Di Rosa P, et al. Prep1 (pKnox1)-deficiency leads to spontaneous tumor development in mice and accelerates EmuMyc lymphomagenesis: a tumor suppressor role for Prep1. *Mol Oncol*. 2010;4(2):126-134.
16. Oriente F, Fernandez Diaz LC, Miele C, et al. Prep1 deficiency induces protection from diabetes and increased insulin sensitivity through a p160-mediated mechanism. *Mol Cell Biol*. 2008;28(18):5634-5645.

17. Oriente F, Cabaro S, Liotti A, et al. PREP1 deficiency down-regulates hepatic lipogenesis and attenuates steatohepatitis in mice. *Diabetologia*. 2013;56(12):2713-2722.

18. Liotti A, Cabaro S, Cimmino I, et al. Prep1 deficiency improves metabolic response in white adipose tissue. *Biochim Biophys Acta*. 2018;1863(5):515-525.

19. Ricci S, Viggiano D, Cimmino I, et al. Prep1 deficiency affects olfactory perception and feeding behavior by impairing BDNF-TrkB mediated neurotrophic signaling. *Mol Neurobiol*. 2018;55(8):6801-6815.

20. Cimmino I, Lorenzo V, Fiory F, et al. A peptide antagonist of Prep1-p160 interaction improves ceramide-induced insulin resistance in skeletal muscle cells. *Oncotarget*. 2017;8(42):71845-71858.

21. Cimmino I, Margheri F, Prisco F, et al. Prep1 regulates angiogenesis through a PGC-1α-mediated mechanism. *FASEB J*. 2019;33(12):13893-13904.

22. Pagano TB, Prisco F, De Biase D, et al. Muscular sarcocystosis in sheep associated with lymphoplasmacytic myositis and expression of major histocompatibility complex class I and II. *Vet Pathol*. 2020;57(2):272-280.

23. Rapa SF, Prisco F, Popolo A, et al. Pro-inflammatory effects of indoxyl sulfate in mice: impairment of intestinal homeostasis and immune response. *Int J Mol Sci*. 2021;22(3):1135.

24. Van Eycke Y-R, Allard J, Salmon I, et al. Image processing in digital pathology: an opportunity to solve inter-batch variability of immunohistochemical staining. *Sci Rep*. 2017;7:42964.

25. Prisco F, De Biase D, Piegari G, et al. Pathologic characterization of white striping myopathy in broiler chickens. *Poult Sci*. 2021;100(7):101150.

26. Chen W-K, Feng L-J, Liu Q-D, et al. Inhibition of leucine-rich repeats and calponin homology domain containing 1 accelerates microglia-mediated neuroinflammation in a rat traumatic spinal cord injury model. *J Neuroinflammation*. 2020;17(1):202.

27. Caporale A, Doti N, Monti A, et al. Automatic procedures for the synthesis of difficult peptides using oxyma as activating reagent: a comparative study on the use of bases and on different deprotection and agitation conditions. *Peptides*. 2018;102:38-46.

28. Lorenzo V, Mascanzoni F, Vitagliano L, et al. The interacting domains of PREP1 and p160 are endowed with a remarkable structural stability. *Mol Biotechnol*. 2016;58(5):328-339.

29. Cimmino I, Oriente F, D'Esposito V, et al. Low-dose bisphenol—a regulates inflammatory cytokines through GPR30 in mammary adipose cells. *J Mol Endocrinol*. 2019;63(4):273-283.

30. De Biase D, Piegari G, Prisco F, et al. Autophagy and NLRP3 inflammasome crosstalk in neuroinflammation in aged bovine brains. *J Cell Physiol*. 2020;235(6):5394-5403.

31. De Biase D, Piegari G, Prisco F, et al. Implication of the NLRP3 inflammasome in bovine age-related sarcopenia. *Int J Mol Scie*. 2021;22(7):3609.

32. Vazquez-Padron RI, Lasko D, Li S, et al. Aging exacerbates neointimal formation, and increases proliferation and reduces susceptibility to apoptosis of vascular smooth muscle cells in mice. *J Vasc Surg*. 2004;40(6):1199-1207.

33. Berthelsen J, Zappavigna V, Mavilio F, et al. Prep1, a novel functional partner of Pbx proteins. *EMBO J*. 1998;17(5):1423-1433.

34. Bailey JS, Rave-Harel N, McGillivray SM, et al. Activin regulation of the follicle-stimulating hormone beta-subunit gene involves Smads and the TALE homeodomain proteins Pbx1 and Prep1. *Mol Endocrinol*. 2004;18(5):1158-1170.

35. Oriente F, Perruolo G, Cimmino I, et al. Prep1, a homeodomain transcription factor involved in glucose and lipid metabolism. *Front Endocrinol*. 2018;9:346.

36. Herzig S, Fuzesi L, Knepel W. Heterodimeric Pbx-Prep1 homeodomain protein binding to the glucagon gene restricting transcription in a cell type-dependent manner. *J Biol Chem*. 2000;275(36):27989-27999.

37. Díaz VM, Mori S, Longobardi E, et al. p160 Myb-binding protein interacts with Prep1 and inhibits its transcriptional activity. *Mol Cell Biol*. 2007;27(22):7981-7990.

38. Monk BA, George SJ. The effect of ageing on vascular smooth muscle cell behaviour—a mini-review. *Gerontology*. 2015;61(5):416-426.

39. McHugh D, Gil J. Senescence and aging: causes, consequences, and therapeutic avenues. *J Cell Biol*. 2018;217(1):65-77.

40. Wang Z, Wei D, Xiao H. Methods of cellular senescence induction using oxidative stress. *Methods Mol Biol*. 2013;1048:135-144.

41. Puzianowska-Kuźnicka M, Owczarz M, Wieczorowska-Tobis K, et al. Interleukin-6 and C-reactive protein, successful aging, and mortality: the PolSenior study. *Immun Ageing*. 2016;13:21.

42. Wei J, Xu H, Davies JL, et al. Increase of plasma IL-6 concentration with age in healthy subjects. *Life Sci*. 1992;51(25):1953-1956.

43. Ershler WB, Sun WH, Binkley N, et al. Interleukin-6 and aging: blood levels and mononuclear cell production increase with advancing age and in vitro production is modifiable by dietary restriction. *Lymphokine Cytokine Res*. 1993;12(4):225-230.

44. Hager K, Machein U, Krieger S, et al. Interleukin-6 and selected plasma proteins in healthy persons of different ages. *Neurobiol Aging*. 1994;15(6):771-772.

45. Kania DM, Binkley N, Checovich M, et al. Elevated plasma levels of interleukin-6 in postmenopausal women do not correlate with bone density. *J Am Geriatr Soc*. 1995;43(3):236-239.

46. Cohen HJ, Pieper CF, Harris T, et al. The association of plasma IL-6 levels with functional disability in community-dwelling elderly. *J Gerontol A Biol Sci Med Sci*. 1997;52(4):M201-M208.

47. Harris TB, Ferrucci L, Tracy RP, et al. Associations of elevated interleukin-6 and C-reactive protein levels with mortality in the elderly. *Am J Med*. 1999;106(5):506-512.

48. Ferrucci L, Corsi A, Lauretani F, et al. The origins of age-related proinflammatory state. *Blood*. 2005;105(6):2294-2299.

49. Lin M-T, Juan C-Y, Chang K-J, et al. IL-6 inhibits apoptosis and retains oxidative DNA lesions in human gastric cancer AGS cells through up-regulation of anti-apoptotic gene mcl-1. *Carcinogenesis*. 2001;22(12):1947-1953.

50. Chen RH, Chang MC, Su YH, et al. Interleukin-6 inhibits transforming growth factor-beta-induced apoptosis through the phosphatidylinositol 3-kinase/Akt and signal transducers and activators of transcription 3 pathways. *J Biol Chem*. 1999;274(33):23013-23019.

51. Klouche M, Bhakdi S, Hemmes M, et al. Novel path to activation of vascular smooth muscle cells: up-regulation of gp130 creates an autocrine activation loop by IL-6 and its soluble receptor. *J Immunol*. 1999;163(8):4583-4589.

52. Watanabe S, Mu W, Kahn A, et al. Role of JAK/STAT pathway in IL-6-induced activation of vascular smooth muscle cells. *Am J Nephrol*. 2004;24(4):387-392.

53. Ikeda U, Ikeda M, Oohara T, et al. Interleukin 6 stimulates growth of vascular smooth muscle cells in a PDGF-dependent manner. *Am J Physiol*. 1991;260(5 Pt 2):H1713-H1717.

54. Ohkawa F, Ikeda U, Kawasaki K, et al. Inhibitory effect of interleukin-6 on vascular smooth muscle contraction. *Am J Physiol*. 1994;266(3 Pt 2):H898-H902.

SUPPORTING INFORMATION

Additional supporting information may be found in the online version of the article at the publisher's website.